Femtosecond fluorescence upconversion studies of intermolecular proton transfer of dipyrido [2,3-a:3?,2?-i] carbazole and related compounds

ARTICLE · JANUARY 2000

5 AUTHORS, INCLUDING:

J. Waluk
Polish Academy of Sciences
256 PUBLICATIONS **3,683** CITATIONS

ARTICLES

(Sub)picosecond Fluorescence Upconversion Studies of Intermolecular Proton Transfer of Dipyrido[2,3-*a*:3′,2′-*i*]carbazole and Related Compounds

D. Marks,[†] H. Zhang,[†] P. Borowicz,[‡] J. Waluk,[‡] and M. Glasbeek*,[†]

Laboratory for Physical Chemistry, University of Amsterdam, Nieuwe Achtergracht 129, 1018 WS Amsterdam, The Netherlands, and Institute of Physical Chemistry, Polish Academy of Sciences, Kasprzaka 44, 01-224 Warsaw, Poland

Received: December 3, 1999; In Final Form: April 25, 2000

For a few carbazole-related compounds in alcoholic solution, photoinduced solute−solvent proton-transfer dynamics are studied by means of femto- and picosecond fluorescence transient measurements. The investigated compounds show two emission bands, the F_1 band (band maximum between 25 500 and 23 000 cm^{-1}) that had previously been attributed to the normal solute−solvent complex and the F_2 band (band maximum between 17 200 and 14 400 cm^{-1}) that had previously been ascribed to the solute−solvent complex in its tautomeric form. Our data show that the F_1 band fluorescence decay contains two fast decay components (the first of these has a time constant between 0.6 and 0.9 ps, the second has a characteristic time between 6.0 and 11 ps) and a slower decay component with a time constant between 50 and 150 ps, depending on the compound and the solvent. The F_2 band shows a fast biexponential rise, which occurs at the same rate as the fast initial decay of the F_1 band emission, followed by a slow decay of about 150−250 ps, depending on the compound and the solvent. The fast decay and rise components of the F_1 and F_2 band emissions, respectively, are discussed as being characteristic of the intermolecular double proton transfer within two distinct "cyclic" solute−solvent complexes. The slower decay component (50−150 ps) in the F_1 band emission is attributed to the decay of the "blocked" solute−solvent complex that does not exhibit intermolecular proton transfer. In deuterated small-molecule alcohols, deuteron transfer is found for one cyclic solute−solvent species only. Its transfer rate appears to be temperature-dependent. The results are suggestive of a thermally averaged deuteron tunneling process in the cyclic solute−solvent complex.

1. Introduction

In recent years, the study of excited-state intermolecular proton transfer has received considerable attention.[1−14] Excited-state proton-transfer reactions are usually initiated by photoinduced changes in the electronic distribution of the reactant molecules. In protic solvents, proton transfer may be facilitated by bridging of the solvent molecules to the reacting solute. For example, 7-hydroxyquinoline[15−17] and 7-azaindole[18−25] show phototautomerization only in protic solvents. In the case of 7-azaindole complexed with alcohol, a single solvent molecule bridges the two molecular sites between which the proton is transferred. For 7-hydroxyquinoline, the distance between the reacting sites is larger, and two solvent molecules or a polymeric matrix are involved in the proton-transfer process.[26−29]

The rate of the reaction can vary considerably among the different systems studied. It has been found for the 7-azaindole dimer in the gas phase that the proton-transfer rate is in the (sub)picosecond range.[30,31] Similar rates have been observed for 7-azaindole dimers dissolved in aprotic solutions.[1,32,33] For 7-azaindole in alcoholic solution, however, the proton-transfer rate is drastically reduced.[18−20] The slowing of the proton transfer has been related to a rearrangement of the solvent molecules prior to the proton transfer; viscosity appears to be an important rate-determining parameter.[18−21] Similarly, for [2,2′-bipyridyl]-3,3′-diol[34] and 3-hydroflavone[35−37] in protic solvents, the rates of the double proton-transfer processes were also found to be solvent-viscosity-dependent.

Solvate structures have been termed "cyclic" and "noncyclic" or "blocked".[3,21] In the cyclic complex of the solute−solvent molecules, the solute molecule is hydrogen-bonded in a cyclic configuration to a single solvent molecule (see e.g., Figure 1). Simulations have shown that, for cyclic structures, very efficient and fast proton-transfer reactions can be expected.[21] Alternatively, the solvate may involve hydrogen bonding between the solute molecules and a chain of solvent molecules in a noncyclic structure or blocked configuration.[3,21] The chain may consist of a wide variety of solvent configurations. In the blocked form, proton transfer is hampered, and a rearrangement of the solvent molecules in the chain is needed to promote the proton transfer.[18,20]

Recently, intermolecular proton transfer has been studied for dipyrido[2,3-*a*:3′,2′-*i*] carbazole (DPC)[38] and its structurally related compounds 1H-pyrrolo[3,2-*h*]quinoline (PQ), 7,8,9,10-

* Correspondence to: Prof. Dr. M. Glasbeek, Laboratory for Physical Chemistry, University of Amsterdam, Nieuwe Achtergracht 129, 1018 WS Amsterdam, The Netherlands.
[†] University of Amsterdam.
[‡] Polish Academy of Sciences.

10.1021/jp994253u CCC: $19.00
Published on Web 07/14/2000

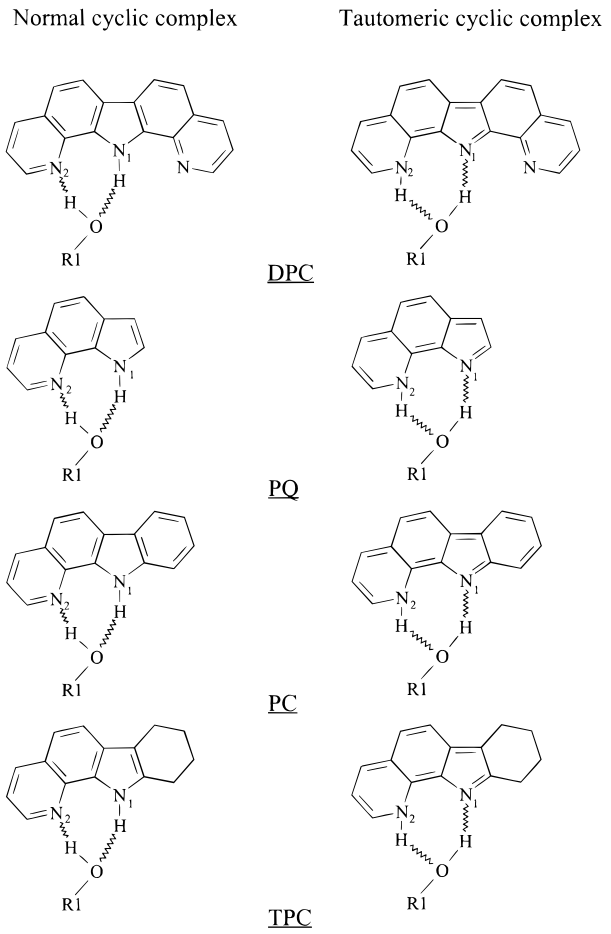

Figure 1. Scheme of the 1:1 solute-alcohol complex for DPC, PQ, PC, and TPC, in both the normal and tautomeric forms.

tetrahydropyrido-[2,3-*a*]carbazole (TPC), and pyrido[2,3,-*a*]-carbazole (PC).[39] For the schematic structures of these molecules, see Figure 1. Two emission bands, with band maxima at 24 500 and 14 800 cm^{-1}, are observed for DPC dissolved in 1-propanol, whereas DPC shows only one emission band (peaking at 25 500 cm^{-1}) when dissolved in *n*-hexane. The band at 24 500 cm^{-1} has been assigned to "normal" DPC (in which no proton has been translocated).[38] The band at 14 800 cm^{-1} is attributed to the tautomer, formed after proton transfer (see top panel of Figure 1). At low temperatures DPC also showed phosphorescence with a band maximum near 19 000 cm^{-1}.[38] In a comparative study of the emission spectra of PQ, TPC, and PC on one hand and model molecules for the "tautomeric" form on the other hand, Kyrychenko et al.[39] concluded that also for these molecules the (low-energy) second-band emission originates from the tautomeric form. It was also concluded that the phosphorescence originates from a blocked complex of the molecule with the solvent molecules. In similar studies by del Valle et al.[40] for PQ and its methylated derivative compound, it was proposed that, in protic solvents, PQ exists in two forms, one of which promotes excited-state double proton transfer catalyzed by a solvent hydrogen bridge, whereas the other mainly gives rise to solvation relaxation in the excited state and subsequent normal fluorescence.

In this paper, we focus on the *dynamics* involved in the fast excited-state intermolecular proton-transfer processes for the molecules DPC, PQ, TPC, and PC in protic solvents. Femto- and picosecond fluorescence measurements are reported for the reactants in various protic solvents. Details concerning the dynamics of the intermolecular proton transfer are obtained from a study of the temporal behavior of the bands characteristic of the normal and tautomeric forms of the solutes. The influence of temperature and deuteration on the intermolecular proton-transfer dynamics is also studied. Finally, results of semiempirical calculations of ground and excited-state energies and the electronic charge redistribution leading to tautomerization are presented and related to the experimental results.

2. Experimental Section

Synthesis of the compounds DPC, PQ, TPC, and PC has been described elsewhere.[41,42] Spectrograde quality ethanol (Merck), 1-propanol (Fluka), and decanol (Aldrich) were used as solvents without further purification. Deuterated ethanol was purchased from Aldrich.

Steady-state absorption spectra were recorded by means of a Shimadzu UV-240 spectrophotometer. The steady-state fluorescence spectra were measured using the emission spectrometer described previously.[43] The emission spectra were corrected for the wavelength-dependent sensitivity of the monochromator−photomultiplier detection system.

Two pulsed-laser setups were used for the measurement of the fluorescence transients: a regeneratively amplified Ti: sapphire laser system with upconversion detection for the time span of 150 fs−100 ps and a picosecond laser system with time-correlated single-photon-counting (TCSPC) detection for the time range of 15 ps−5 ns. The systems have been described in detail previously.[43,44] In the femtosecond laser system, excitation was accomplished by laser pulses (∼100 fs) from an OPA system in the range of 310−350 nm (∼0.1 μJ/pulse). An attenuated part of the fundamental beam (800 nm) was led through an optical delay line and focused, together with the pump-pulse-induced fluorescence, onto a 1-mm thick BBO crystal (type I phase-matching condition). The upconversion signal (at the sum frequency of the fluorescence and the fundamental of the femtosecond laser) was focused on the entrance slit of a monochromator and photodetected by means of a photomultiplier. The time resolution of the upconversion experiment, as deduced from the fwhm of the cross-correlation signal of the gating and OPA laser beams, is approximately 150 fs. To avoid detection of kinetics due to reorientational motions, the gating beam was polarized at a magic angle with respect to the excitation beam.

In the picosecond fluorescence setup, photoexcitation was fixed at 322 nm by means of picosecond pulses of about 7 ps (fwhm autocorrelation trace) and 25 nJ at 3.7 MHz. The fluorescence emitted from the sample in a direction perpendicular to the excitation beam was focused onto the entrance slit of a monochromator outfitted with a multichannel-plate photodetector. A linear polarizer was inserted in the detection pathway to detect at magic-angle conditions. The instrumental response time was about 17 ps (fwhm).

The temperature dependence of the fluorescence transients in the range from 170 to 300 K was studied using the picosecond fluorescence setup. The quartz cuvette containing the solution was mounted inside a home-built nitrogen flow cryostat outfitted with regulated temperature control. The temperature was measured with a thermocouple attached to the cuvette holder.

All calculations were performed with the SPARTAN 5.0 software packet. The initial geometry of the molecule was optimized for minimum energy by molecular mechanics calculations using the Merck force field. The result of this optimization was employed as input data for RHF/PM3 semiempirical calculations[45] for further optimization of the molecular structure. Optimization was ended once default criteria for

TABLE 1: Position of Band Maxima in Absorption and Emission Spectra for the Indicated Compounds Dissolved in Ethanol

	absorption (cm^{-1})	emission (cm^{-1})	
		F_1 band	F_2 band
DPC	28 800	25 060	15 100
PQ	30 100	25 500	17 200
TPC	28 550	23 500	16 050
PC	29 400	23 400	14 440

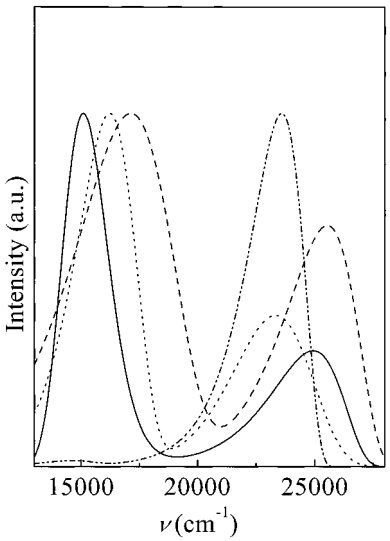

Figure 2. Steady-state fluorescence spectra of DPC (solid line), PQ (dashed line), TPC (dotted line), and PC (dashed−dotted line), dissolved in ethanol.

convergence were reached. For the optimized molecular structure, excited-state energies and charge distributions were obtained after configuration interaction (CI). In the latter, the basis set configurations consisted of excitations from the seven highest-occupied SCF molecular orbitals (HOMOs) to the seven lowest-unoccupied molecular orbitals (LUMOs).

3. Results

3.1. DPC. The continuous-wave (cw) absorption spectrum of DPC in protic solvents has been reported by Herbich et al.[38] The lowest absorption band for the molecule dissolved in ethanol has its maximum at 28 800 cm^{-1}. The absorption bands are shifted slightly to the red as the polarity of the solvent increases. The emission spectrum of DPC varies depending on the solvent. In aprotic solvents, the emission spectrum consists of a single emission band having a maximum near 25 500 cm^{-1}. This emission band is labeled F_1. In protic solvents, two emission bands are observed, the F_1 band (in ethanol, its maximum is at 25 060 cm^{-1}) and the F_2 band, positioned to the red with respect to the F_1 band (in ethanol, its maximum is at 15 100 cm^{-1}). The absorption and emission band positions for the solute dissolved in ethanol are summarized in Table 1. Figure 2 shows the cw emission spectrum for DPC dissolved in ethanol.

Previously, the emission results have been explained on the basis of a solvent-mediated intermolecular proton transfer for DPC in the excited state.[38] The F_1 band emission has been assigned as the radiative decay of the initially excited state, while the F_2 band has been attributed to the tautomeric form after the excited-state double proton transfer (see scheme in Figure 1). The proposed scheme is corroborated by the results of semiempirical calculations.[38]

We have measured the time dependence of the F_1 and the F_2 band emissions. Typical transients in the femtosecond fluorescence upconversion measurements, detected at the wavelengths of the F_1 and the F_2 band emissions of DPC in 1-propanol, are presented in Figure 3. The time behavior of the two emission bands is quite different. When detection is within the F_1 band (Figure 3a), the fluorescence transient consists of an instantaneous rise followed by a decay on the picosecond time scale. After deconvolution with the system response function, the decay detected at 443 nm could be best fit to a triexponential decay function

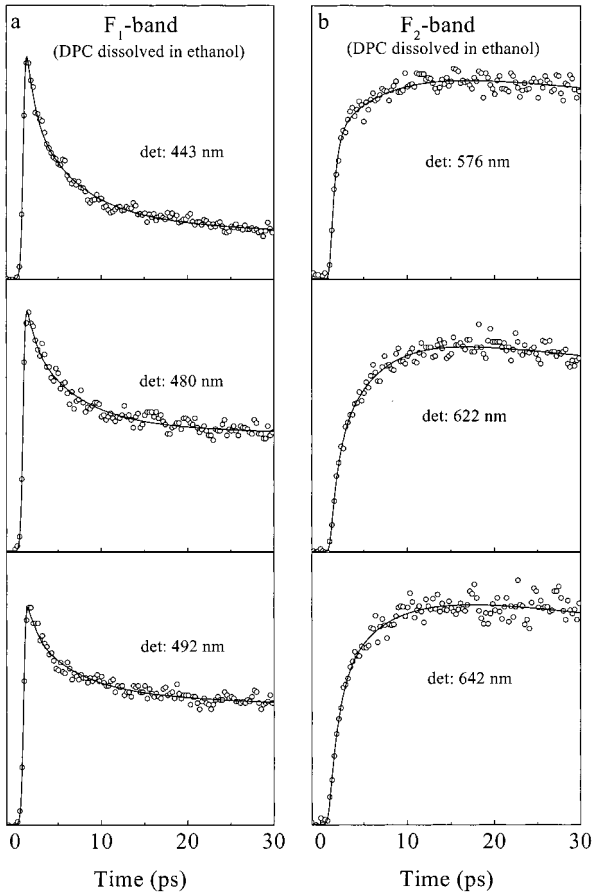

Figure 3. Fluorescence transients of DPC (in 1-propanol) detected at the wavelengths indicated. (a) Transients for F_1 emission band and (b) transients for F_2 emission band. Solid lines are best fits to multiexponential functions specified in text convoluted with the system response function.

$$I(F_1, t) = A_1(F_1)\exp[-t/\tau_1(F_1)] + A_2(F_1)\exp(-t/\tau_2(F_1)] + A_3(F_1)\exp(-t/\tau_3(F_1)] \quad (1)$$

in which $\tau_1(F_1) = 0.8 \pm 0.5$ ps, $\tau_2(F_1) = 6.0 \pm 1.0$ ps, and $\tau_3(F_1) = 170 \pm 10$ ps. It appeared that fitting to a biexponential function gave a less good fit (in particular because the initial fluorescence intensity could not be fully simulated), whereas fitting with a multiexponential function containing more than three components did not yield better fits. Thus, we limit ourselves to fitting to a triexponential function. Table 2 summarizes the characteristic times thus obtained for the F_1 band emission of DPC dissolved in various alcohols. For detection wavelengths lower than 440 nm, the relative weights of the three components are also indicated. Transients detected within the F_2 emission band (Figure 3b) initially exhibit a rise component followed by a decay. After deconvolution with the system response function, the transient fit a triexponential function of the form

TABLE 2: Time Constants for the F_1 and F_2 Emission Bands of DPC in Various Alcohols

	F_1 band			F_2 band		
DPC dissolved in	$\tau_1(F_1)$ (ps)	$\tau_2(F_1)$ (ps)	$\tau_3(F_1)$ (ps)	$\tau_1(F_2)$ (ps)	$\tau_2(F_2)$ (ps)	$\tau_3(F_2)$ (ps)
methanol	0.7 (0.21)	7.0 (0.56)	75 (0.22)	0.7 (−0.38)	7.0 (−0.62)	150 (1.0)
ethanol	0.7 (0.23)	7.0 (0.40)	77 (0.17)	0.7 (−0.4)	7.0 (−0.6)	178 (1.0)
1-propanol	0.8 (0.28)	6.0 (0.36)	170 (0.36)	0.8 (−0.5)	6.0 (−0.5)	206 (1.0)
decanol	0.9 (0.40)	7.0 (0.34)	700 (0.26)	0.9 (−0.41)	7.0 (−0.59)	330 (1.0)
methanol-*d*	9.0[a] (0.65)		20.0 (0.35)	9.0[a] (−1.0)		207 (1.0)
ethanol-*d*	8.5[a] (0.60)		45 (0.40)	9.5[a] (−1.0)		306 (1.0)

[a] corresponds to τ_D.

$$I(F_2, t) = A_1(F_2)\exp[-t/\tau_1(F_2)] + A_2(F_2)\exp(-t/\tau_2(F_2)] + A_3(F_2)\exp(-t/\tau_3(F_2)] \quad (2)$$

where $\tau_1(F_2) = 0.8 \pm 0.5$ ps, $\tau_2(F_2) = 6.0 \pm 1.0$ ps, and $\tau_3(F_2) = 206 \pm 10$ ps (cf Table 2). Experimentally, the longer decay time, τ_3, was reproduced in the fluorescence transient measurements by means of the TCSPC setup, using a time window of 5 ns.

It is noted that the 0.8- and 6.0-ps decay components in the F_1 band match the two rise times of the F_2 band. Following the assignment of Herbich et al.,[38] that the F_1 emission is due to the initially excited normal form and the F_2 emission to the tautomeric form, we will argue in section 4 that, for DPC in 1-propanol, the kinetics of proton transfer in its excited state are given by the time constants τ_1 and τ_2 and thus can be resolved in time. Here we note simply that the proton-transfer time constants, τ_1 and τ_2 (cf Table 2) are within the upper limit of about 10 ps estimated for the first proton-transfer step in 7-hydroxyquinoline,[15] but they are much faster than the proton-transfer time of 226 ps for 7-azaindole in 1-propanol.[18]

For DPC dissolved in methanol, ethanol, and decanol, quite similar fluorescence transients were measured. From the best fits to eqs 1 and 2, the values for the characteristic decay and rise times listed in Table 2 were obtained. The times τ_1 andτ_2 (characteristic of proton transfer, see section 4) at room temperature are again found to be near 0.8 and 7.0 ps, irrespective of the nature of the solvent.

Using *deuterated* alcoholic solvents, the fluorescence transients slowed down. Typical transients measured for DPC dissolved in protonated and deuterated methanol at room temperature are displayed in Figure 4 (upper panels of a and b). The results for the best-fit values of the time constants for DPC in deuterated methanol are included in Table 2. Note that, now, only a biexponential (instead of a triexponential) decay (with characteristic times τ_D and τ_3) is observed for the transients detected at the F_1 emission wavelengths.

At lower temperatures, τ_1 and τ_2 for DPC in *protonated* liquid 1-propanol is not noticeably affected (within the limited time resolution of the picosecond TCSPC experiments). The long-time components, $\tau_3(F_1)$ and $\tau_3(F_2)$, are found to increase as the temperature is lowered. For example, at a temperature of 210 K, we find $\tau_3(F_1) = 510 \pm 20$ ps and $\tau_3(F_2) = 410 \pm 20$ ps. In *deuterated* methanol, however, the influence of temperature on τ_D is appreciable. When the temperature is lowered, τ_D is found to increase. An Arrhenius plot of $\ln(1/\tau_D)$ against $1/T$ for DPC in deuterated methanol is included in Figure 5. Also, the longer decay components slow down. For example, at 190 K, the decay time becomes, $\tau_3(F_1) = 710 \pm 20$ ps.

3.2. TPC. The lowest absorption band for TPC dissolved in ethanol has a maximum near 28 550 cm^{-1}. The cw emission spectra of TPC are similar to those of PQ and DPC. In aprotic solvents, only a single emission band, labeled F_1, exists. In acetonitrile, the emission band maximum is near 23 000 cm^{-1}.[39]

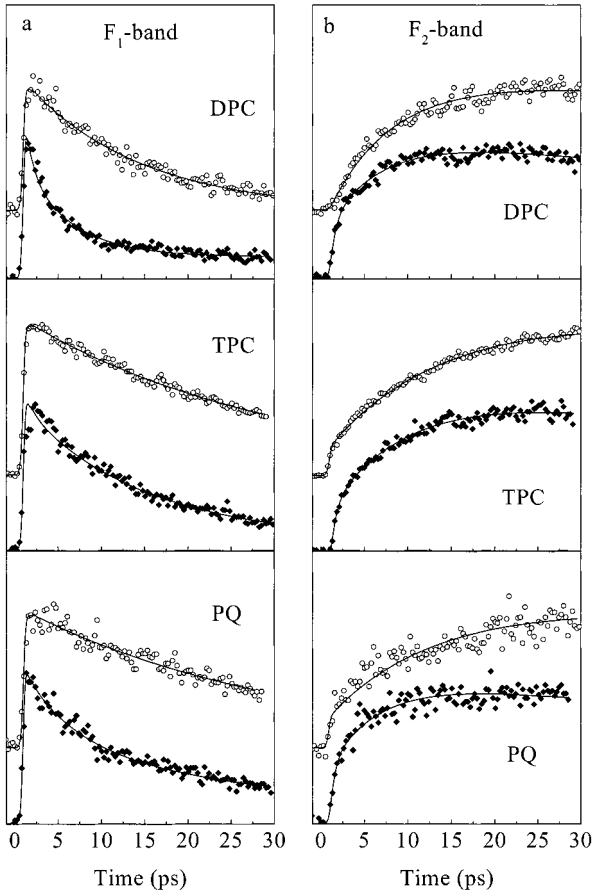

Figure 4. Fluorescence transients for DPC, TPC, and PQ dissolved in protonated ethanol (filled diamonds) and deuterated ethanol (open circles). (a) Detection at the F_1 emission band and (b) detection at the F_2 emission band. Solid lines are best fits to function indicated in text convoluted with system response function.

In protic solvents, two emission bands are observed. In ethanol, the F_1 band has its maximum near 23 500 cm^{-1}, and the F_2 band emission peaks at 16 050 cm^{-1}. Figure 2 displays the cw emission spectrum for TPC dissolved in ethanol. Previously, the F_1 band has been attributed to emission from the initially excited state, while the F_2 band was assigned to the tautomer formed after the double proton transfer (see scheme in Figure 1).[39]

The time dependence of both bands was measured. The fluorescence transients of TPC in 1-propanol are similar to those described in the previous sections. The results for the time constants of TPC in various alcohol solvents as obtained from the fittings (performed as before) are collected in Table 3. The typical times for τ_1 and τ_2 are 0.8 and 10.0 ps, respectively. The eventual decay of the F_1 and F_2 emissions occurs with values for $\tau_3(F_1)$ of about 30−130 ps and for $\tau_3(F_2)$ of about 140−300 ps, depending on the solvent. Typical fluorescence upconversion transients for TPC in ethanol, 1-propanol and

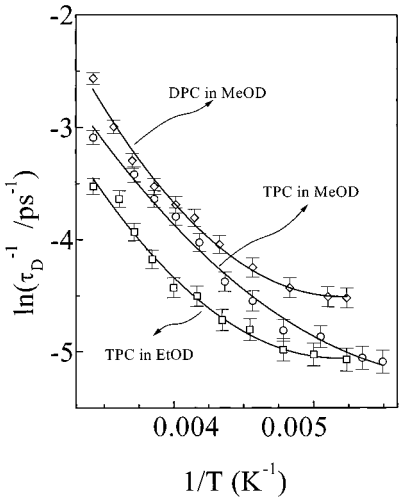

Figure 5. Plot of $\ln(1/\tau_D)$, with τ_D in picoseconds, versus $1/T$ (with T in Kelvin) of DPC and TPC in deuterated methanol and TPC in deuterated ethanol.

decanol are displayed in Figure 6. Table 3 includes the relative weights of the various rise and decay components.

In *deuterated* methanol and ethanol at room temperature, the F_1 band decay of TPC is biexponential with a τ_D value of about 20−30 ps, the F_2 band shows a rise with the same time constant, followed by a decay with a time constant, $\tau_3(F_2)$, of about 200−240 ps. Figure 4 shows a few illustrative transients for TPC dissolved in protonated and deuterated ethanol at room temperature. When the temperature is decreased, only for the deuterated solutions could a change in the deuteron transfer rate be resolved with the TCSPC picosecond setup. In Figure 5, Arrhenius plots for the time constant, $\ln(1/\tau_D)$ versus $1/T$, for TPC in deuterated methanol and ethanol solutions are presented. Also, an increase in the longer decay time, $\tau_3(F_2)$, is found as the temperature is decreased. At 190 K, for TPC in protonated ethanol, we have $\tau_3(F_1) = 150 \pm 20$ ps and $\tau_3(F_2) = 250 \pm 20$ ps. At the same temperature, for TPC dissolved in deuterated ethanol, we find $\tau_3(F_1) = 500 \pm 20$ ps.

The influence of the excitation wavelength on the fluorescence time dependence was also investigated. At excitation wavelengths ranging from 310 to 350 nm, the fluorescence kinetics remained unchanged. This is in contrast to the situation reported for 7-azaindole dimers in the gas phase for which the proton-transfer time was found to vary with the excitation wavelength.[30]

3.3. PQ. The cw absorption and emission spectra of PQ in protic solvents have been discussed by Kyrychenko et al.[39] and by del Valle et al.[40] The lowest absorption band of PQ dissolved in ethanol has its maximum at 30 100 cm^{-1}. As in the case of DPC in aprotic solvents, the emission spectrum of PQ consists of a single emission band labeled F_1. In acetonitrile, for example, the emission maximum is centered at 25 850 cm^{-1}. In protic solvents, two emission bands are observed, the F_1 band (in ethanol, the band maximum is at 25 500 cm^{-1}) and the F_2 band at lower energy (in ethanol, the band maximum is at 17 200 cm^{-1}). The data are summarized in Table 1. Figure 2 shows the cw emission spectrum for PQ dissolved in ethanol.

As for DPC, the emission bands have been related to solvent-mediated intermolecular proton transfer in the excited state of PQ.[39,40] The F_1 band emission has been assigned as the radiative decay of the initially excited state, while the F_2 band has been attributed to the tautomeric form obtained after the excited-state double proton transfer (see scheme in Figure 1).

As for DPC, we have measured the time dependence of the F_1 and the F_2 band emissions for PQ. Transients obtained in the femtosecond fluorescence upconversion measurements for PQ dissolved in 1-propanol, detected at wavelengths within the F_1 and the F_2 bands, are very similar to those of DPC presented in Figure 3. For detection within the F_1 band, the fluorescence transient of PQ consists of an instantaneous rise followed by a decay on the picosecond time scale. Fitting the transients to a triexponential decay function, in a fashion similar to that mentioned in section 3.1, we obtain the time constants presented in Table 4. For detection wavelengths below 430 nm, the relative weights of the three components are included in the table. Transients detected within the F_2 emission band exhibit initially a biexponential rise, with time constants equal to the decay constants of the F_1 band, followed by a decay of several hundred picoseconds. The longer decay times, $\tau_3(F_1)$ and $\tau_3(F_2)$, were determined by measurement of the fluorescence transients with the fluorescence TCSPC setup using a time window of 5 ns.

In *deuterated* ethanol, at room temperature, as for DPC and TPC, the F_1 band decay of PQ is biexponential with a value for the τ_D time of approximately 20−30 ps; the F_2 band shows a rise of 20−30 ps followed by a decay of approximately 250−300 ps. Figure 4 shows a few illustrative transients for PQ dissolved in protonated and deuterated ethanol at room temperature. When the temperature is decreased, the same behavior as for DPC and TPC was observed. Only for the deuterated solutions could a change in the proton-transfer rate be resolved with the TCSPC picosecond setup. An increase in the longer decay times, $\tau_3(F_1)$ and $\tau_3(F_2)$, is found as the temperature is decreased. At 190 K, for PQ in protonated ethanol we have, $\tau_3(F_1) = 290 \pm 20$ ps, $\tau_3(F_2) = 550 \pm 20$ ps. At the same temperature, for PQ dissolved in deuterated ethanol, we find $\tau_3(F_1) = 1150 \pm 20$ ps.

3.4. PC. The lowest absorption band of this molecule has a maximum near 29 400 cm^{-1}. The emission spectrum consists mainly of one band with a maximum at 23 400 cm^{-1} for the molecule dissolved in ethanol. A second, much weaker, emission band, with a maximum near 14 440 cm^{-1}, has been reported by Kyrychenko et al.[39] This band is just barely noticeable in the cw emission spectrum of PC presented in Figure 2.

The time dependence of the F_1 emission band was measured for PC dissolved in methanol, ethanol, 1-propanol and decanol. The fluorescence transients fit a single-exponential decay function with the characteristic decay times as listed in Table 5. Because of its low intensity, the temporal behavior of the F_2 band emission could not be measured.

4. Discussion

It is recalled that the F_1 and F_2 band emissions, observed for DPC, PQ, and TPC in alcoholic solution, originate from the photoexcited molecules before and after the solvent-mediated double proton transfer.[39] In section 3, it was shown for all of the investigated molecules that the time constants, τ_1 and τ_2, that are typical of the initial F_1-band decay turn out to be equal to the time constants that characterize the biexponential rise of the F_2 band emission. Evidently, the times τ_1 and τ_2 are somehow related to the proton-transfer process. The question then arises whether the finding of two times (τ_1 and τ_2) automatically implies a two-step intermolecular double proton-transfer process. The answer is negative. This can be deduced from the biexponential fast decay in the F_1 band emission (with time constants τ_1 and τ_2). Neither in a simple one-step nor in a two-step mechanism would a biexponential decay behavior for the F_1 band emission be expected: both mechanisms would give

TABLE 3: Time Constants for the F_1 and F_2 Emission Bands of TPC in Various Alcohols

	F_1 band			F_2 band		
TPC dissolved in	$\tau_1(F_1)$ (ps)	$\tau_2(F_1)$ (ps)	$\tau_3(F_1)$ (ps)	$\tau_1(F_2)$ (ps)	$\tau_2(F_2)$ (ps)	$\tau_3(F_2)$ (ps)
methanol	0.9 (0.19)	11.0 (0.45)	30 (0.36)	0.9 (−0.30)	11.0 (−0.7)	138 (1.0)
ethanol	0.8 (0.35)	11.0 (0.37)	50 (0.28)	0.8 (−0.44)	11.0 (−0.6)	157 (1.0)
1-propanol	0.7 (0.48)	10.0 (0.30)	58 (0.20)	0.7 (−0.46)	10.0 (−0.5)	187 (1.0)
decanol	0.7 (0.46)	8.5 (0.32)	133 (0.21)	0.7 (−0.42)	8.5 (−0.58)	300 (1.0)
methanol-*d*	19.0[a] (0.50)		35 (0.50)	18.5[a] (−1.0)		205 (1.0)
ethanol-*d*	34.0[a] (1.0)		−	34.0[a] (−1.0)		240 (1.0)

[a] corresponds to τ_D.

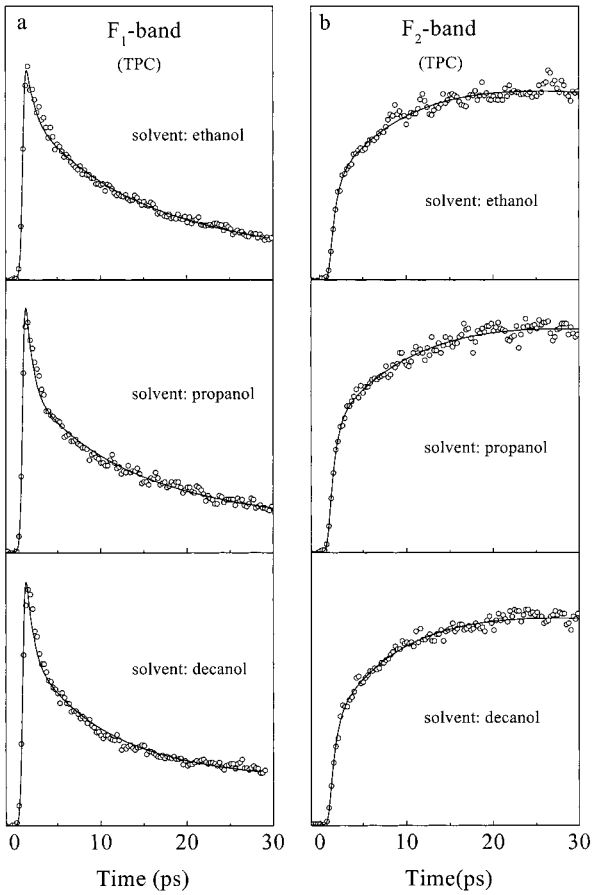

Figure 6. Fluorescence transients of TPC in different alcoholic solvents. (a) Detection at 460 nm and (b) detection at 620 nm. Solid lines show best fit to multiexponential functions specified in text convoluted with the system response function.

rise to a single decay step for the initially excited species and thus lead to a single-exponential decay of the F_1 band emission. Because this is not found experimentally, we infer that the double-exponential F_1 band decay (and the concomitant F_2 band rise) must reflect the concurrent presence of two distinct solute−solvent species that may differ slightly in structure, but that each give rise to a single double proton-transfer time (τ_1 and τ_2). It is noted in passing that, for DPC, PQ, and TPC, the tautomerization process differs from that discussed very recently for 7-azaindole (7-AI) in nonpolar solvents.[1] For the latter molecule it was found that, at room temperature, sequential as well as concerted double proton transfer occurs. However, in the case of 7-AI a pronounced probe- and detection-wavelength dependence for the kinetics was found in the transient absorption and femtosecond fluorescence transient measurements, respectively. In the fluorescence transient measurements for the probe molecules investigated in this paper, a wavelength dependence for τ_1 and τ_2, representative of excited-state nuclear dynamics, could not be resolved.

For the fluorescent molecules studied, excited-state proton transfer is accomplished through hydrogen bonding to nearby solvent molecules.[38,39] In cases in which the probe molecule is hydrogen-bonded to a single solvent molecule at two sites (see scheme in Figure 1), the solute−solvent complex is cyclic. Generally, in the cyclic configuration, the proton-transfer process is optimized. Another possibility would be that the solute is hydrogen-bonded to a chain of solvent molecules in a noncyclic structure, i.e., a blocked configuration.[3,21] The chain may then involve a wide variety of solvent configurations. In some instances, a conversion between the blocked and cyclic forms is a determining factor in the proton-transfer rate.[18,20] By means of molecular dynamics simulations, Mente and Maroncelli[21] calculated that, in ethanol, the fraction of complexes in a cyclic position is much higher for DPC than for 7-azaindole. Similar conclusions were reached by Kyrychenko et al.[39] for PQ. As is evident from Tables 2−5, the proton-transfer times, τ_1 and τ_2, are only very slightly dependent on the alcoholic solvent or its viscosity. Thus, in line with the behavior predicted from the calculations,[21,39] we propose for DPC and its related compounds that only configurations that, prior to excitation, are already in the cyclic configuration, are involved in the proton-transfer process. Note that, in each of the two structurally slightly different species, there is a single proton-transfer time (given by τ_1 or τ_2), as manifested by the synchronous F_1 decay and F_2 rise. Thus, in each of the species there is just one excited-state proton transfer. Most likely, therefore, the two protons that are transferred in the excited state of the two structurally slightly different species are translocated concurrently, and no intermediate state is involved. This is in contrast with 7-hydroxyquinoline, in which the creation of an intermediate state is reported.[15]

The decay component of the F_1 band fluorescence with the characteristic time $\tau_3(F_1)$ is attributed to the decay of blocked complexes. The magnitude of $\tau_3(F_1)$ is probe-molecule-, solvent-, and temperature-dependent. The short lifetime of the excited state of the blocked conformation is representative of an efficient nonradiative decay out of the fluorescent state, and thus, proton transfer in this configuration remains unobserved. It is remarkable that this short decay is observed only in protic solvents and only in compounds that possess both proton-donor and proton-acceptor groups. Assuming similar oscillator strengths and spectral positions for the absorption and fluorescence from the blocked and cyclic configurations, the relative concentration of the blocked configurations is estimated as, $[A_3(F_1)*\tau_3(F_1)]/[A_1(F_1)*\tau_1(F_1) + A_2(F_1)*\tau_2(F_1) + A_3(F_1)*\tau_3(F_1)]$ (ref 46). With the values for the weight factors given in section 3, we thus obtain values of 0.72, 0.83, and 0.65 for the relative concentration of the blocked configurations of DPC, PQ, and TPC, respectively, in methanol. These values are of the same order of magnitude as those reported elsewhere.[39] We note in passing that the cyclic and blocked forms do not interconvert during the excited-state lifetime. If this occurred, then there would be only one decay time for both species, instead of the measured

TABLE 4: Time Constants for the F_1 and F_2 Emission Bands of PQ in Various Alcohols

	F_1 band			F_2 band		
PQ dissolved in	$\tau_1(F_1)$ (ps)	$\tau_2(F_1)$ (ps)	$\tau_3(F_1)$ (ps)	$\tau_1(F_2)$ (ps)	$\tau_2(F_2)$ (ps)	$\tau_3(F_2)$ (ps)
methanol	0.6 (0.14)	6.0 (0.46)	41 (0.39)	0.6 (−0.36)	6.0 (−0.64)	170 (1.0)
ethanol	0.7 (0.19)	9.0 (0.56)	76 (0.24)	0.7 (−0.62)	9.0 (−0.38)	230 (1.0)
1-propanol	0.7 (0.16)	7.0 (0.37)	87 (0.47)	0.7 (−0.46)	7.0 (−0.5)	270(1.0)
decanol	0.9 (0.37)	9.0 (0.23)	300 (0.40)	0.9 (−0.66)	9.0 (−0.34)	413 (1.0)
methanol-*d*	19.0[a] (0.50)		32 (0.50)	23.0[a] (−1.0)		245 (1.0)
ethanol-*d*	32.0[a] (1.0)		50 (0.55)	32.0[a] (−1.0)		327 (1.0)

[a] corresponds to τ_D.

TABLE 5: Time Constant for the F_1 Emission Band of PQ in Various Alcohols

PC dissolved in	τ_P (ps)
methanol	15
ethanol	30
propanol	50

TABLE 6: Atomic Distances and Molecular Energies as Calculated by the Semi-Empirical Methods Mentioned in the Text

		distances (Å)		energies (kcal/mol)			
		$r(N_1-O)$	$r(N_2-O)$	HOMO	LUMO	CI (ground state)	CI (excited state)
DPC	normal	2.76	2.75	−8.14	−0.80	20.7	82.6
	tautomer	2.67	2.77	−7.57	−1.71	46.5	80.9
PQ	normal	2.76	2.75	−8.47	−0.59	−19.6	37.0
	tautomer	2.68	2.78	−7.85	−1.49	7.2	38.7
TPC	normal	2.76	2.75	−8.25	−0.55	−33.5	24.9
	tautomer	2.68	2.78	−7.59	−1.44	−9.0	21.6
PC	normal	2.77	2.76	−8.09	−0.80	−4.2	55.1
	tautomer	2.67	2.78	-−7.48	−1.62	19.6	44.6

τ_1 or τ_2 time constants, on one hand, and $\tau_3(F_1)$ time constant on the other hand.

As illustrated in Figure 5, the excited-state proton-transfer times when deuterated methanol and ethanol are used show a temperature dependence. Several possibilities for the interpretation of this temperature dependence can be considered. For instance, one might consider that the orientation of the solvent molecule with respect to the solute in the cyclic complex undergoes some adjustment in order to facilitate the proton/deuteron transfer. In this instance, one can imagine that the viscosity of the solvent would be of influence to the reorientation dynamics. However, although the viscosities of deuterated and undeuterated ethanol are slightly different[47] [their ratio, $\eta_r = \eta_D/\eta_H$, at room temperature, is always smaller than 1.13 (ref 47)], this ratio is too small to account for the slowing of the deuteron-transfer process by more than a factor 4 in going from the protonated to the deuterated solution. Alternatively, tunneling might be considered for the discussion of the decrease in the proton-transfer rate in deuterated ethanol. Specifically, deuteration of the solvent would affect the deuteron transfer rate in the cyclic complex. The thermally averaged deuteron-tunneling rate would become smaller as the temperature was lowered.[48,49] This would qualitatively explain why the values of the $\ln(1/\tau_D)$ data points in Figure 5 show a decrease with an increasing value of $1/T$.

The data points in Figure 5 show Arrhenius behavior for $T > 220$ K, but at lower temperatures there is a deviation from this behavior. This is not uncommon for tunneling systems.[48,49] We therefore consider that the data points can be fit to a function of the form[48]

$$\ln(k) = (-E_a/k_B T) + \ln[A^* Q_t(T)] \quad (3)$$

where Q_t is the tunneling correction function. For a parabolic barrier, Q_t is given by

$$Q_t(T) = [{}^1/_2 * u]/[\sin({}^1/_2 * u)] \quad (4)$$

where $u = h\nu_‡/k_B T$ and $\nu_‡$ is the imaginary frequency of the barrier.[48]

The best fits of the experimental results for DPC and TPC to eq 3 appear as the drawn curves in Figure 5. These fits yield, for DPC in methanol, an activation energy of $E_a = 9.7$ kcal/mol and an imaginary frequency of $\nu_‡ = 6.9 \times 10^{13}$ s^{-1} and, for TPC in methanol, an activation energy of $E_a = 7.7$ kcal/mol and an imaginary frequency of $\nu_‡ = 5.8 \times 10^{14}$ s^{-1}. Likewise, also for nondeuterated alcohols, a slowing of the proton-transfer time at lower temperatures is expected. However, as mentioned in section 3, a temperature dependence for τ_1 or τ_2 could not be resolved for the undeuterated solutions. If τ_1 or τ_2 is increased by a factor of 3 to 4 when $T = 190$ K (similar to the deuteron case, although the increase factor is usually much smaller[48]), then at 190 K, a maximum value for the proton-transfer time of about 15 ps (for DPC in protic ethanol) is expected. With the TCSPC setup (used in the fluorescence transient experiments at the lower temperatures), this time constant is just at the edge of the experimental time resolution, and thus, it may well be that the temperature effect in the undeuterated ethanol solution could not be resolved. Another feature supportive of the idea that the proton-transfer rate is determined by tunneling is the finding that τ_1 and τ_2 in the protonated solvents are solvent-independent.

We have also performed some simulations of the structure of a 1:1 cyclic complex of the solute−solvent system in the ground state, using the geometry optimization method of RHF/PM3.[45] As mentioned above, the experimental data show that the proton-transfer rate for the 1:1 cyclic solvate does not change with the choice of the protic solvent. Thus, for the sake of simplicity, in the calculations, the model solvent molecule in the complex was chosen to be methanol. It was verified that, when the methanol molecule is replaced by 1-propanol, the simulation results were not affected. For the cyclic 1:1 solvates of DPC, PQ, and PC, the calculations predicted planar molecular structures, as expected for conjugated systems. Geometry optimization calculations were performed for both the normal and tautomeric forms (see Figure 1) of DPC, PQ, TPC and PC. The calculated distance between the oxygen atom of the solvent molecule and the nitrogen atoms (N_1 and N_2) of the solute molecule for both the normal and tautomeric species are presented in Table 6. When the structures of the considered complexes in the normal and tautomeric forms are compared, it is noted that the distance between the N_1 atom and the solvent oxygen atom decreases by about 0.08 Å and the distance between the N_2 atom and the solvent oxygen atom increases by about 0.02 Å. From this, it is inferred that the proton transfer may be accompanied by a slight reorientation of the solvent

TABLE 7: Calculated Charges at Positions N_1 and N_2

		charge N_1		charge N_2		δ
		ground state	excited state	ground state	excited state	excited state
DPC	normal	0.348	0.512	−0.086	−0.191	0.703
	tautomer	−0.164	−0.003	0.486	0.251	−
PQ	normal	0.337	0.474	−0.097	−0.239	0.713
	tautomer	−0.175	−0.098	0.405	0.229	−
TPC	normal	0.350	0.415	−0.098	−0.202	0.617
	tautomer	−0.162	−0.130	0.394	0.232	−
PC	normal	0.266	0.465	−0.085	−0.215	0.680
	tautomer	−0.225	−0.024	0.539	0.287	−

molecule, thereby making the proton transfer, in fact, a multidimensional process.

The driving force for the proton-transfer process becomes apparent from the results of the energy calculations. Restricted Hartree−Fock energy calculations were performed for DPC, PQ, TPC and PC, each in the normal and tautomeric forms. The energies of the corresponding HOMOs and LUMOs are presented in Table 6. For each of the molecules considered, the energy of the HOMO of the normal form is lower than that of its analogue for the tautomeric form. The opposite is found for the energies of the LUMO, for which the energies in the normal form are higher than those in the tautomeric form. The calculations indicate that, in the ground state, the normal form is lower in energy, and thus, in alcoholic solution, this form is dominant. In the excited state, the tautomeric form is stabilized with respect to the normal form, thus leading to tautomerization. Results of CI calculations confirm this picture. The CI energies of the ground and lowest excited states are included in Table 6. For each molecule, the ground-state configuration energy in the normal form is considerably lower than that in its tautomeric form. With the exception of PQ, the energy of the tautomer in its first excited state is lower than for the normal species in the first excited state. It is remarked that, as the basis set of excited configurations in the CI calculation is increased, the excited-state energy of the tautomeric form is decreased even more. Thus, the CI calculations also show that, in the ground state, the normal form is lower in energy, and thus, in alcoholic solution, this form is dominant. In the excited state, the tautomeric form is stabilized with respect to the normal form, thus leading to tautomerization. Previous calculations reported elsewhere yielded similar conclusions.[38,39] It should be added, however, that the quantitative agreement between the CI results and the experimental optical transition energies is rather poor, although the calculations predict similar absorption energies for the DPC, PQ and PC molecules. Thus, the calculations are valuable for qualitative purposes only.

Finally, Table 7 includes the Mulliken charge distribution after CI at the nitrogen atom sites, N_1 and N_2. It is noted from the table that, in the normal form , the charge at atomic site N_1 increases appreciably after excitation. At the same time, the charge at atomic site N_2 becomes more negative. A similar enhanced acidity/basicity after excitation has been treated elsewhere also.[26,50] The charge redistribution in the molecule after excitation underlies the proton-transfer process. Our calculations (Table 7) illustrate that photoexcitation results in an appreciable value of δ (i.e., the charge difference, in the excited state, of atoms N_1 and N_2). The calculated values for δ indicate that impulsive photoexcitation induces appreciable changes in the electronic charge distribution and that the chromophores exhibit excited-state proton transfer rather than H-atom transfer. If, on the other hand, excited-state H-atom transfer would be more appropriate than proton transfer for the studied chromophores, then the electronic charge distribution would adiabatically adjust to the movements of the protons. One might intuitively expect a correlation between the proton-transfer rate and the amount of electronic charge redistribution. Indeed, the calculated smaller extent of the electronic redistribution as manifested by δ for TPC is in line with the experimentally determined lower rate of excited-state tautomerization in this molecule in comparison with DPC and PQ. It should be added, though, that other factors such as molecular size or the presence of nearby excited states should also be taken into account when such a rate−structure relationship is considered.

For similar activation energies for proton tunneling in cyclic complexes of TPC, DPC, and PQ, the excited-state proton transfer in TPC is predicted to be slower than those of DPC or PQ. This prediction is borne out by the experimental results.

5. Conclusion

In previous studies of the molecules under investigation, it had been proposed, on the basis of their spectroscopic behavior in aprotic and protic solvents, that the F_1 and F_2 band emissions originate from different species: the F_1 band is characteristic of the normal form of the solute−solvent complex and the F_2 band is due to the tautomer form of the cyclic solute−solvent complex. The time-resolved experiments presented in this paper provide independent additional evidence for the model. Whereas the F_1 band emission shows a picosecond biexponential decay [with time constants $\tau_1(F_1)$ and $\tau_2(F_1)$], the F_2 band emission shows a fast biexponential rise, with the same time constants. It has been argued that there are two distinct solute−solvent cyclic species in which the two protons at sites N_1 and N_2 are transferred simultaneously. (A dark intermediate of extremely short lifetime, much less than 500 fs, is unlikely.) For the two species, the proton-transfer times (τ_1 and τ_2) could be determined (Tables 2−5). The time-resolved experiments also provide evidence for the existence of a longer-lived noncyclic species [with a lifetime of $\tau_3(F_1)$], not involved in a fast excited-state proton-transfer process. This species is associated with the blocked solute−solvent form. Finally, the proton-transfer rate ($1/\tau_D$) for the probe molecules in deuterated solvents was found to be slightly temperature-dependent. It was discussed that the temperature effect is indicative of a thermally averaged proton-tunneling process in the cyclic complex. The results of semiempirical calculations suggest a slight modification of the structure of the cyclic complex as the double proton transfer takes place.

Acknowledgment. The research was financially supported by the Council for Chemical Sciences of The Netherlands Organization for Scientific Research (CW-NWO). One of us (D.M.) gratefully acknowledges discussions with Dr. A. M. Brouwer in performing the semiempirical calculations. P.B and J.W. acknowledge the support from the U.S.−Polish Maria Skłodowska-Curie Joint Fund II (Grant 97-305).

References and Notes

(1) Fiebig, T.; Chachisvilis, M.; Manger, M.; Zewail, A. H.; Douhal, A.; Garcia-Ochoa, I.; de La Hoz Ayuso, A. *J. Phys. Chem A* **1999**, *103*, 7419.

(2) Guallar, V.; Batista, V. S.; Miller, W. H. *J. Chem. Phys.* **1999**, *110*, 9922.

(3) Herbich, J.; Hung, C.-Y.; Thummel, R. P.; Waluk, J. *J. Am. Chem. Soc*. **1996**, *118*, 3508.

(4) Goodman, M. F. *Nature* **1995**, *378*, 237.

(5) Douhal, A.; Guallar, V.; Moreno, M.; Lluch, J. M. *Chem. Phys. Lett*. **1996**, *256*, 370.

(6) Naik, D. B.; Dwibedy, P.; Dey, G. R.; Kishore, K.; Moorthy, P. N. *J. Phys. Chem. A* **1998**, *102*, 684.

(7) Marx, D.; Tuckerman, M. E.; Hutter, J.; Parrinello, M. *Nature* **1999**, *397*, 601.
(8) Hynes, J. T. *Nature* **1999**, *397*, 565.
(9) Lopez-Matinez, R.; Long, P.; Solgadi, D.; Soep, B.; Syage, J.; Millie, P. *Chem. Phys. Lett*. **1997**, *273*, 219.
(10) Mosquera, M.; Penado, J. C.; Riós Rodrígues, M. C.; Rodrígues-Prieto, F. *J. Phys. Chem.* **1996**, *100*, 5398.
(11) Huang, Y.; Arnold, S.; Sulkes, M. *J. Phys. Chem*. **1996**, *100*, 4734.
(12) Bardez, E.; Chatelain, A.; Larrey, B.; Veleur, B. *J. Chem. Phys*. **1994**, *98*, 2357.
(13) Nakajima, A.; Hirano, M.; Hasumi, R.; Kaya, K.; Watanabe, H.; Carter, C. C.; Williamson, J. M.; Miller, T. A. *J. Phys. Chem. A* **1997**, *101*, 392.
(14) Smirnov, A. V.; English, D. S.; Rich, R. L.; Lane, J.; Teyton, L.; Schwabacher, A. W.; Luo, S.; Thornburg, R. W.; Petrich, J. W. *J. Phys. Chem B* **1997**, *101*, 2758.
(15) Lee, S.-I.; Jang, D.-J. *J. Phys. Chem*. **1995**, *99*, 7537.
(16) Kim, T.-G.; Lee, S.-I.; Jang, D.-J.; Kim, Y. *J. Chem. Phys.* **1995**, *99*, 12698.
(17) Tokumura, K.; Natsume, M.; Nakagawa, T.; Hashimoto, M.; Yuzawa, T.; Hamaguchi, H.; Itoh, M. *Chem. Phys. Lett*. **1997**, *271*, 320.
(18) Konijnenberg, J.; Huizer, A. H.; Varma, C. A. G. O. *J. Chem. Soc., Faraday Trans. 2* **1988**, *84*, 1163
(19) Herbich, J.; Sepiol, J.; Waluk, J. *J. Mol. Struct.* **1984**, *114*, 329
(20) Chapman, C. F.; Maroncelli, M. *J. Phys. Chem*. **1992**, *96*, 8430.
(21) Mente, S.; Maroncelli, M. *J. Phys. Chem. A* **1998**, *102*, 3860.
(22) Chen, Y.; Gai, F.; Petrich, J. W. *J. Am. Chem. Soc.* **1993**, *115*, 10158.
(23) Chen, Y.; Gai, F.; Petrich, J. W. *Chem. Phys. Lett*. **1994**, *222*, 329.
(24) Chang, C.-P.; Wen-Chi, H.; Meng-Shin, K.; Chou, P.-T, Clements, J. H. *J. Phys. Chem*. **1994**, *98*, 8801.
(25) Chou, P.-T.; Wei, C.-Y.; Chang, C.-P.; Meng-Shin, K. *J. Phys. Chem*. **1995**, *99*, 11994.
(26) García-Ochoa, I.; Bisht, P. B.; Sánchez, F.; Martinez-Atáz, E.; Santos, L.; Tripathi, H. B.; Douhal, A. *J. Phys. Chem. A* **1998**, *102*, 8871.
(27) Douhal, A.; Sastre, R. *Chem. Phys. Lett.* **1994**, *219*, 91.
(28) Lahmani, F.; Douhal, A.; Breheret, E.; Zehnacker-Rentien, A. *Chem. Phys. Lett.* **1994**, *220*, 235.
(29) Douhal, A.; Dabrio, J.; Sastre, R. *J. Phys. Chem*. **1996**, *100*, 149.
(30) Douhal, A.; Kim, S. K.; Zewail, A. H. *Nature* **1995**, *378*, 260.
(31) Folmer, D. E.; Poth, L.; Wisniewski, E. S.; Castleman A. W. Jr. *Chem. Phys. Lett.* **1998**, *287*, 1.
(32) Takeuchi, S.; Tahara, T. *J. Phys. Chem. A* **1998**, *102*, 7740.
(33) Chachisvilis, M.; Fiebig, T.; Douhal, A.; Zewail, A. H. *J. Phys. Chem. A* **1998**, *102*, 669.
(34) Marks, D.; Zhang, H.; Glasbeek, M.; Borowicz, P.; Grabowska, A. *Chem. Phys. Lett.* **1997**, *275*, 370.
(35) Strandjord, A. J. G.; Barbara, P. F. *J. Phys. Chem*. **1985**, *89*, 2355.
(36) Brucker, G. A.; Kelley, D. F. *J. Phys. Chem*. **1987**, *91*, 2856.
(37) Schwartz, B. J.; Peteanu, L. A.; Harris, C. B. *J. Phys. Chem*. **1992**, *96*, 3591.
(38) Herbich J.; Dobkowski, J.; Thummel R. P.; Hegde, V.; Waluk, J. *J. Phys. Chem. A* **1997**, *101*, 5839.
(39) Kyrychenko, A.; Herbich, J.; Izydorzak, M.; Wu, F.; Thummel, R. P.; Waluk, J. *J. Am. Chem. Soc.* **1999**, *121*, 11179.
(40) Del Valle, J. C.; Domínguez, E.; Kasha, M. *J. Phys. Chem. A* **1999**, *103*, 2467.
(41) Hegde, V.; Hung, C.-Y.; Madhukar, P.; Cunningham, R.; Höpfner, T.; Thummel, R. P. *J. Am. Chem. Soc*. **1993**, *115*, 872.
(42) Wu, F.; Hardesty, J.; Thummel, R. P. *J. Org. Chem*. **1998**, *63*, 4055.
(43) Middelhoek, E. R.; van der Meulen, P.; Verhoeven, J. W.; Glasbeek, M. *Chem. Phys*. **1995**, *198*, 573.
(44) Prosposito, P.; Marks, D.; Zhang, H.; Glasbeek, M. *J. Phys. Chem. A* **1998**, *102*, 8894.
(45) Stewart, J. J. P. *The Encyclopedia of Computational Chemistry*; von Ragùe Schleyer, P., Ed.; John Wiley & Sons: Chichester, U.K., 1998; pp 2080−2086.
(46) Wei, C.-Y.; Yu, W.-S.; Chou, P.-T.; Hung, F.-T.; Chang, C.-P.; Lin, T.-C. *J. Phys. Chem. B* **1998**, *102*, 1053.
(47) Holz, M.; Mao, X.; Seiferling, D. *J. Chem. Phys*. **1996**, *104*, 669.
(48) Bell, R. P. *The Tunnel Effect in Chemistry*; Chapman and Hall: New York, 1980.
(49) Tokumura, K.; Watanabe, Y.; Udagawa, M.; Itoh, M. *J. Am. Chem. Soc.* **1987**, *109*, 1346.
(50) Bardez, E.; Devol, I.; Larrey, B.; Valeur, B. *J. Phys. Chem. B* **1997**, *101*, 7786.